



This is a repository copy of *High permittivity and low loss microwave dielectrics suitable for 5G resonators and low temperature co-fired ceramic architecture*.

White Rose Research Online URL for this paper:
<http://eprints.whiterose.ac.uk/122935/>

Version: Accepted Version

Article:

Zhou, D., Pang, L.X., Wang, D.W. et al. (3 more authors) (2017) High permittivity and low loss microwave dielectrics suitable for 5G resonators and low temperature co-fired ceramic architecture. *Journal of Materials Chemistry C*, 5 (38). pp. 10094-10098.

<https://doi.org/10.1039/c7tc03623j>

Reuse

Items deposited in White Rose Research Online are protected by copyright, with all rights reserved unless indicated otherwise. They may be downloaded and/or printed for private study, or other acts as permitted by national copyright laws. The publisher or other rights holders may allow further reproduction and re-use of the full text version. This is indicated by the licence information on the White Rose Research Online record for the item.

Takedown

If you consider content in White Rose Research Online to be in breach of UK law, please notify us by emailing eprints@whiterose.ac.uk including the URL of the record and the reason for the withdrawal request.



eprints@whiterose.ac.uk
<https://eprints.whiterose.ac.uk/>

High permittivity, low loss microwave dielectrics suitable for 5G resonator and low temperature co-fired ceramic architecture

Di Zhou^{*a,b}, Li-Xia Pang^{a,c}, Da-Wei Wang^a, Chun Li^d, Biao-Bing Jin^d & Ian M. Reaney^{*a}

^aDepartment of Materials Science and Engineering, University of Sheffield, S1 3JD,
UK

^bElectronic Materials Research Laboratory, Key Laboratory of the Ministry of Education & International Center for Dielectric Research, Xi'an Jiaotong University, Xi'an 710049, Shaanxi, China

^cMicro-optoelectronic Systems Laboratories, Xi'an Technological University, Xi'an 710032, Shaanxi, China

^dResearch Institute of Superconductor Electronics (RISE), School of Electronic Science and Engineering, Nanjing University, Nanjing, Jiangsu, 210093, China.

*Corresponding author E-mail address: i.m.reaney@sheffield.ac.uk (Ian M. Reaney) & zhoudi1220@gmail.com (Di Zhou)

Abstract

$\text{Bi}_2(\text{Li}_{0.5}\text{Ta}_{1.5})\text{O}_{7+x}\text{Bi}_2\text{O}_3$ ($x=0, 0.01$ and 0.02) ceramics were prepared using a solid state reaction method. All compositions crystallized in a single $\text{Bi}_2(\text{Li}_{0.5}\text{Ta}_{1.5})\text{O}_7$ phase without secondary peaks in X-ray diffraction patterns. $\text{Bi}_2(\text{Li}_{0.5}\text{Ta}_{1.5})\text{O}_7$ ceramics densified at $1025\text{ }^\circ\text{C}$ with a permittivity (ϵ_r) ~ 65.1 , $Qf \sim 15,500\text{ GHz}$ ($Q \sim$ microwave quality factor; $f \sim$ resonant frequency; $16,780\text{ GHz}$ when annealed in O_2) and temperature coefficient of resonant frequency (TCF) $\sim -17.5\text{ ppm}/^\circ\text{C}$. The sintering temperature was lowered to $\sim 920\text{ }^\circ\text{C}$ by the addition of 2 mol. % excess Bi_2O_3 ($\epsilon_r \sim 64.1$, a $Qf \sim 11,200\text{ GHz}$ / $11,650\text{ GHz}$ when annealed in O_2 and a TCF $\sim -19\text{ ppm}/^\circ\text{C}$) with compositions chemically compatible with Ag electrodes. $\text{Bi}_2(\text{Li}_{0.5}\text{Ta}_{1.5})\text{O}_{7+x}\text{Bi}_2\text{O}_3$ are ideal for applications as dielectric resonators in 5G mobile base station technology for which ceramics with $60 < \epsilon_r < 70$, high Qf and close to zero TCF are commercially unavailable. They may additionally prove useful as high ϵ_r , high Qf materials in low temperature co-fired ceramic (LTCC) technology.

I. Introduction

Microwave (MW) dielectric ceramics have been used in mobile communications, satellite television broadcasts, radar, Global Position System (GPS), Wireless Fidelity (WiFi) and other modern communication systems as dielectric resonator (DR), filters, duplexers and substrates, for almost half a century due to their high dielectric permittivity (ϵ_r), **high Qf (Q ~ MW quality factor and f ~ resonant frequency) and small** temperature coefficient of resonant frequency (TCF).¹⁻⁶ Since the first report of MW dielectrics in the BaO-TiO₂ binary system,^{7,8} **ceramics with a range of ϵ_r , high Qf and near-zero TCF such as the** Ba(Zn,Mg,Co)_{1/3}(Nb,Ta)_{2/3}O₃, (Sr,Ca)TiO₃-LnAlO₃ (Ln=La, Nd, Sm), (Zr,Sn)TiO₄ and BaO-Ln₂O₃-TiO₂⁸⁻¹⁵ have been developed for use from 300 MHz ~ 40 GHz by **leading corporations such as Murata, Kyocera, EPCOS and Trans-Tech.**¹⁶⁻¹⁹ In general, the roadmap for the **development of** MW dielectric materials^{2-4,6} may be separated into the following key target areas where there is a technology pull from systems engineers and the absence suitable materials:

- i) Expanding the range of ϵ_r . Currently, most high Qf, zero TCF materials have $20 < \epsilon_r < 50$ (base station resonators/antenna substrates) but there is a strong technology pull for $5 < \epsilon_r < 20$ (higher bandwidth antenna substrates), $60 < \epsilon_r < 70$ (base station resonators) and $\epsilon_r > 120$ (ultra-small GPS antenna substrates).
- ii) Low sintering temperature technology. The drive is to create a range of low temperature co-fired ceramics (LTCC) compatible with Ag electrodes (sintering temperature **~960 °C**) or ultra-low temperature co-fired ceramics (ULTCC) compatible with Al as inner electrodes (sintering temperature < 660 °C).
- iii) Ultrahigh Qf ceramics ($>200,000$ GHz).**The** focus here is to optimize Qf to

achieve better selectivity to a specific frequency, critical for the transition from 4G to 5G technology in mobile telecommunications.

- iv) Compositions based on low cost, abundant constituents. Here, the technology is driven by scarcity, environmental concerns and geopolitical uncertainty surrounding raw materials such as Ta₂O₅, Nb₂O₅, and Ln₂O₃ (Ln = lanthanide).

Generically, MW dielectric ceramics are oxides, principally due to the large ionic polarizability of the O²⁻ ion.²⁰ Binary compounds, such as MgO, TiO₂, Bi₂O₃, TeO₂, Al₂O₃ and CeO₂,²¹⁻²⁶ possess high Qf and in some cases useful ϵ_r but invariably have large positive/negative TCF. Hence, ternary and higher compounds or composites are often explored to obtain temperature stable microwave dielectric ceramics with high Qf.¹⁻¹⁵ The key to success in MW ceramic development is therefore in choosing, either an adaptable crystal structure to form solid solutions or immiscible end members to form composites that have no or limited interaction. Perovskite is the most adaptable crystal structure to form solid solution for MW ceramics (ABO₃) since a large number of metallic elements may occupy the A and B sites in accordance with the Goldschmidt tolerance factor,²⁷

$$t = (R_A + R_B) / \sqrt{(R_B + R_O)}, \quad (1)$$

where R_A, R_B and R_O are the ionic radii of the A-, B- and O-site. Perovskites dominate medium and high permittivity commercial MW dielectrics in the range $25 < \epsilon_r < 60$ and $\epsilon_r > 90$.⁸⁻¹³ Although efforts have been made to explore novel complex perovskite-structured microwave dielectrics with $\epsilon_r \sim 65$, only limited progress has been achieved with $Qf < 12,500$ GHz.²⁸ Moreover, it is difficult to lower the sintering temperatures of perovskites and related microwave dielectrics to meet the requirements of LTCC technology. For example, commercial tungsten bronze structured compounds achieve $70 < \epsilon_r < 90$ and $8,000 < Qf < 12,000$ GHz¹⁹ when

sintered to full density. If the sintering temperature is lowered to ~ 900 °C by the addition of glass, ϵ_r and Qf decrease to ~ 65 and $< 6,000$ GHz, respectively.²⁹ Despite the great potential of LTCC technology and a substantial body of work in the scientific literature, suppliers such as Dupont and Ferro offer only a limited range of commercial LTCC materials.^{30,31}

In the present work, we have synthesized quaternary compounds in the $\text{Bi}_2(\text{Li}_{0.5}\text{Ta}_{1.5})\text{O}_{7+x}\text{Bi}_2\text{O}_3$ ($x = 0, 0.01$ and 0.02) which are suitable for use as both dielectric resonators for 5G, targeting applications which require $60 < \epsilon_r < 70$, and also in LTCC technology with ceramics with $x = 0.02$ compatible with Ag electrodes.

II. Experimental section

Sample preparation. Reagent-grade Li_2CO_3 ($> 99\%$, Fisher Scientific), Bi_2O_3 , ($> 99\%$, Sigma-Aldrich) and Ta_2O_5 ($> 99\%$, Fisher Scientific) were weighed according to the stoichiometric formulation $\text{Bi}_2(\text{Li}_{0.5}\text{Ta}_{1.5})\text{O}_{7-x}\text{Bi}_2\text{O}_3$ ($x = 0, 0.01$ and 0.02). Powders were mixed and ball-milled for 24 h using isopropanol. The powder mixture was then dried and calcined 4 h at 750 °C. The calcined powders were re-milled for 24 h and hand pressed into cylinders (13 mm in diameter and 4 ~ 5 mm in height) at 50 MPa. **Samples were sintered 2h at 880 °C ~ 1040 °C and annealed at optimal sintering temperatures in N_2 , air and O_2 atmospheres.**

Characterization and electrical measurements. X-ray diffraction (XRD) was performed using with $\text{CuK}\alpha$ radiation (Bruker D2 Phaser) from 5 - 80 ° 2θ at a step size of 0.02 °. The results were analyzed by the Rietveld profile refinement method, using the FULLPROF program. As-fired and fractured surfaces were observed by scanning electron microscopy (SEM, FEI, Inspect F). The dielectric properties over 0.2 to 1.2 THz (6.7 – 40 cm^{-1}) were measured by terahertz time-domain (THz TDS) spectroscopy (ADVAVTEST TAS7500SP, Japan). A passive mode-lock fiber laser is used to pump

and gate respectively two GaAs photoconductive antennas for the generation and detection of THz wave. Profiles of electric field of THz pulses were measured with and without the sample as a reference. Fourier transformation was applied to obtain the complex transmission coefficient and the index of refraction was extracted through the Fresnel formula. Dielectric properties at MW frequency were measured with the TE_{01δ} dielectric resonator method with a network analyzer (Advantest R3767CH; Advantest, Tokyo, Japan) and a home-made heating system. The temperature coefficient of resonant frequency TCF (τ_f) was calculated with the following formula:

$$\text{TCF}(\tau_f) = \frac{f_{85} - f_{25}}{f_{25} \times (85 - 25)} \times 10^6 \quad (2)$$

where f_{85} and f_{25} are the TE_{01δ} resonant frequencies at 85 °C and 25 °C, respectively.

III. Results and discussions

Figure 1 shows the XRD patterns of Bi₂(Li_{0.5}Ta_{1.5})O_{7+x}Bi₂O₃ (x = 0, 0.01 and 0.02) ceramics sintered at different temperatures and co-fired with 30 wt. % silver powder. As reported by Muktha et al.,³² undoped Bi₂(Li_{0.5}Ta_{1.5})O₇ crystalize in a variant of the Aurivillius structure with a monoclinic, C2/c space group. The diffraction peaks from 415141-ICSD (Inorganic Crystal Structure Database) are also plotted in Figure 1. All peaks were attributed to a single Bi₂(Li_{0.5}Ta_{1.5})O₇ phase when sintered at their optimal temperatures with no evidence of second phase, despite the addition of excess Bi₂O₃. Although it is possible that excess Bi₂O₃ becomes incorporated in the lattice, Bi-rich phases may also exist but below the detection limit of the XRD equipment used within this study. Results from Rietveld structural refinements are shown in Figure S1 of the supplementary material.

The addition of 2 mol. % Bi₂O₃ lowers the sintering temperature from 1025 °C to

920 °C, below the melting point of Ag (~ 961 °C) which raises the possibility that $\text{Bi}_2(\text{Li}_{0.5}\text{Ta}_{1.5})\text{O}_7$ based ceramics may be suitable for LTCC technology, provided that no reaction occurs. As seen from Figure 1, only peaks of $\text{Bi}_2(\text{Li}_{0.5}\text{Ta}_{1.5})\text{O}_7$ and silver were observed in the ceramic co-fired with Ag powder sintered at 920 °C. The absence of secondary phases in XRD therefore suggests that $\text{Bi}_2(\text{Li}_{0.5}\text{Ta}_{1.5})\text{O}_7+0.02\text{Bi}_2\text{O}_3$ ceramics are chemically compatible with Ag.

Secondary electron (SE) images of the $\text{Bi}_2(\text{Li}_{0.5}\text{Ta}_{1.5})\text{O}_7+x\text{Bi}_2\text{O}_3$ ($x = 0, 0.01$ and 0.02) ceramics sintered at their optimal temperatures, BSE images of $\text{Bi}_2(\text{Li}_{0.5}\text{Ta}_{1.5})\text{O}_7+0.02\text{Bi}_2\text{O}_3$ co-fired at 920 °C with Ag powder and an electrode, and a schematic of the crystal structure of $\text{Bi}_2(\text{Li}_{0.5}\text{Ta}_{1.5})\text{O}_7$ are shown in Figure 2. Dense, homogenous microstructures were revealed for all the ceramics, Figure 2(a) – (c) with the grain size of $\text{Bi}_2(\text{Li}_{0.5}\text{Ta}_{1.5})\text{O}_7+x\text{Bi}_2\text{O}_3$ ($x = 0, 0.01$ and 0.02) decreasing from ~ 5 to ~ 3 μm for $x = 0$ and $x = 0.02$, respectively, presumably due to the reduction in sintering temperature.

The theoretical density of $\text{Bi}_2(\text{Li}_{0.5}\text{Ta}_{1.5})\text{O}_7$ is reported by Muktha³² as 9.002 g/cm^3 and confirmed from the XRD results present in this study. Bulk densities of $\text{Bi}_2(\text{Li}_{0.5}\text{Ta}_{1.5})\text{O}_7+x\text{Bi}_2\text{O}_3$ ceramics sintered at their optimal temperatures were 8.782 g/cm^3 , 8.826 g/cm^3 , and 8.873 g/cm^3 for $x = 0, 0.01$ and 0.02 , respectively, and thus relative densities > 97 % were achieved for all compositions. The BSE image of ceramics co-fired with $\text{Bi}_2(\text{Li}_{0.5}\text{Ta}_{1.5})\text{O}_7+0.02\text{Bi}_2\text{O}_3$ and silver powders and with a Ag surface electrode are shown in Figure 2 (d) and (e). The silver grains have a lower weight average atomic number than $\text{Bi}_2(\text{Li}_{0.5}\text{Ta}_{1.5})\text{O}_7+0.02\text{Bi}_2\text{O}_3$ and thus appear darker. There is no evidence of a reaction zone at the Ag/ $\text{Bi}_2(\text{Li}_{0.5}\text{Ta}_{1.5})\text{O}_7+0.02\text{Bi}_2\text{O}_3$ interface. Moreover, a dense microstructure and clean interface is observed between the Ag electrode and

ceramic in Figure 2(e). The SEM images therefore, confirm XRD results that $\text{Bi}_2(\text{Li}_{0.5}\text{Ta}_{1.5})\text{O}_7+0.02\text{Bi}_2\text{O}_3$ ceramics are chemically compatible with Ag and thus suitable for LTCC technology.

Microwave dielectric properties of the $\text{Bi}_2(\text{Li}_{0.5}\text{Ta}_{1.5})\text{O}_7+x\text{Bi}_2\text{O}_3$ ($x = 0, 0.01$ and 0.02) ceramics as a function of sintering temperature are presented in Figure 3. ϵ_r and Qf of $\text{Bi}_2(\text{Li}_{0.5}\text{Ta}_{1.5})\text{O}_7$ increased from 62.5 to 65.1 and 13,820 to 15,500 GHz, respectively, as sintering temperature increased from 1000 °C to 1025 °C and then decreased slightly, possibly due to either secondary grain growth and/or volatilization of Bi_2O_3 . After annealing 2h in O_2 at 1000 °C, Qf was improved to 16,780 GHz which is attributed to the decrease in oxygen vacancies (V_{O}). Meanwhile, Qf of samples annealed in N_2 decreased slightly. Generally, the improvements in Qf due to a decrease in V_{O} when annealed in O_2 are limited to < 8 %. A similar trend was observed for $\text{Bi}_2(\text{Li}_{0.5}\text{Ta}_{1.5})\text{O}_7+0.01\text{Bi}_2\text{O}_3$ but we note that the densification temperature decreased from ~ 1000 to ~ 975 °C.

For $x=0.02$, ϵ_r and Qf decreased to 64.1 and ~11,200 GHz (11,650 GHz after annealing in O_2), respectively, but sintered at 920 °C, accompanied by a decrease in TCF from - 17.5 to - 19 ppm/°C. Although TCF requires further tuning to obtain values closer to zero, possibly through the substitution of Nb for Ta or addition of typical microwave dielectric with large positive TCF, such as TiO_2 or CaTiO_3 , the MW properties demonstrate proof of concept that $\text{Bi}_2(\text{Li}_{0.5}\text{Ta}_{1.5})\text{O}_7+x\text{Bi}_2\text{O}_3$ ceramics have the potential for commercial exploitation in resonator and LTCC applications.

In the microwave region, polarizability is the sum of both ionic and electronic components. Shannon²⁰ suggested that molecular polarizability(α) of complex substances may be estimated by summing α of the constituent ions which for $\text{Bi}_2(\text{Li}_{0.5}\text{Ta}_{1.5})\text{O}_7$ is:

$$\alpha_{\text{Bi}_2(\text{Li}_{0.5}\text{Ta}_{1.5})\text{O}_7} = 2\alpha_{\text{Bi}^{3+}} + 0.5\alpha_{\text{Li}^+} + 1.5\alpha_{\text{Ta}^{5+}} + 7\alpha_{\text{O}^{2-}} \approx 34.01 \text{ \AA}^3, \quad (3)$$

where the ionic polarizabilities of Bi^{3+} , Li^+ , Ta^{5+} and O^{2-} are 6.12 \AA^3 , 1.20 \AA^3 , 4.73 \AA^3 and 2.01 \AA^3 , respectively.²⁰ Considering the Clausius–Mosotti relation,³³

$$\varepsilon_{\text{meas}} = \frac{3V + 8\pi\alpha}{3V - 4\pi\alpha} \Rightarrow \alpha = \frac{3V(\varepsilon - 1)}{4\pi(\varepsilon + 2)} \approx 33.71 \text{ \AA}^3, \quad (4)$$

where V is the cell volume ($1182.61/8 = 147.826 \text{ \AA}^3$), the molecular polarizability may be obtained from ε_r to give $\sim 33.71 \text{ \AA}^3$ which is similar to the calculated value (34.01 \AA^3) based on Shannon's additive rule.

The complex permittivity of $\text{Bi}_2(\text{Li}_{0.5}\text{Ta}_{1.5})\text{O}_7$ ceramics measured at MW frequencies using $\text{TE}_{01\delta}$ method and THz region using THz-TDS technology (Terahertz time domain spectroscopy)^{34,35} are plotted as a function frequency in Figure 4. Complex refractivity (n^*) can be obtained from the THz transmission data without using the Kramers-Kronig relation.³⁴⁻³⁶ From the relation between refractivity and ε ($\sqrt{\varepsilon^*} = n^*$), the real and imaginary part of ε may be calculated. As shown in Figure 4, the real part of ε for $\text{Bi}_2(\text{Li}_{0.5}\text{Ta}_{1.5})\text{O}_7$ increased from ~ 65 at 200 GHz (similar to the measured value at 4.3 GHz) to ~ 76 at 1100 GHz before decreasing sharply, implying that the first phonon oscillation absorption occurred at 1100 GHz, possibly associated with the stretching mode of the Bi-O bond. The imaginary part of ε also followed a similar trend. ε obtained from THz-TDS technology and $\text{TE}_{01\delta}$ resonance method are thus in good agreement.

Qf of commercial microwave dielectric ceramics as a function of ε_r are plotted in Figure 5a. Qf and ε_r of $\text{Bi}_2(\text{Li}_{0.5}\text{Ta}_{1.5})\text{O}_7$ ceramics effectively fill the gap in resonator technology for $60 < \varepsilon_r < 70$ where previously no high Qf materials ($> 15,000 \text{ GHz}$) have been reported. Moreover, we note that commercial MW ceramics such as $\text{CaTiO}_3\text{-NdAlO}_3$ have been fabricated for a number of years in large volumes and

the extrinsic dielectric losses minimized by tailored dopants and processing. We propose that Qf of $\text{Bi}_2(\text{Li}_{0.5}\text{Ta}_{1.5})\text{O}_7$ may thus be improved in the future by the use of appropriate dopants and by superior synthesis methods. The sintering temperatures and microwave dielectric properties of high ϵ_r (> 60) single phase LTCC materials are listed in Table 1 with Qf versus ϵ_r plotted in Fig. 5b. We note that Qf of pyrochlore $\text{Bi}_2(\text{Zn}_{1/3}\text{Ta}_{2/3})_2\text{O}_7$, Li-Nb-Ti-O M-phase and Bi_2O_3 -CaO-Nb₂O₅ system are inferior to $\text{Bi}_2(\text{Li}_{0.5}\text{Ta}_{1.5})\text{O}_7+0.02\text{Bi}_2\text{O}_3$ (11,200 GHz).³⁷⁻⁴² Given the low sintering temperature of $\text{Bi}_2(\text{Li}_{0.5}\text{Ta}_{1.5})\text{O}_7+0.02\text{Bi}_2\text{O}_3$ and its compatibility with Ag, we propose that it offers an ideal solution for high Qf, ϵ_r materials in LTCC technology ($\epsilon_r \sim 64.1$, a Qf $\sim 11,200$ GHz and a TCF ~ -19 ppm/°C). The above discussions are based on ceramics sintered from single monolithic green bodies. We note that stacking ceramics with adhesive bonding is also an effective way to achieve near-zero TCF materials over a wide range of permittivities.⁴³ However, this latter route offers limited control over resonator geometry.

IV. Conclusions

The $\text{Bi}_2(\text{Li}_{0.5}\text{Ta}_{1.5})\text{O}_7$ ceramic sinter to $> 95\%$ theoretical density at 1125 °C with $\epsilon_r \sim 65.1$, Qf $\sim 15,500$ and TCF ~ -17 ppm/°C, filling the gap in ϵ_r between 60 \sim 70 for base station resonators application. Furthermore, annealing in O₂ further increased Qf to 16,780 GHz. The sintering temperature of the based composition is lowered to 920 °C by adding 2 mol. % Bi₂O₃ whilst retaining excellent MW dielectric properties, $\epsilon_r \sim 64.1$, Qf $\sim 11,200$ GHz (almost twice larger than the existing LTCCs with the similar permittivity) and TCF ~ -19 ppm/°C. In conclusion, these compositions occupy a unique place in the pantheon of microwave ceramics and have the potential to attain commercial exploitation as either 5G resonators and/or in LTCC technology.

Acknowledgements

This work was supported by Sustainability and Substitution of Functional Materials and Devices EPSRC (EP/L017563/1), the National Natural Science Foundation of China (U1632146), the Young Star Project of Science and Technology of Shaanxi Province (2016KJXX-34), the Key Basic Research Program of Shaanxi Province (2017GY-129), the Fundamental Research Funds for the Central University, and the 111 Project of China (B14040).

References

1. R. D. Richtmyer, *J. Appl. Phys.* 1939, **10**, 391.
2. M. Mirsaneh, O. P. Leisten, B. Zalinska, I. M. Reaney, *Adv. Funct. Mater.* 2008, **18**, 2293.
3. M. T. Sebastian, R. Uvic, H. Jantunen, *Int. Mater. Rev.* 2015, **60**, 392.
4. M. T. Sebastian, H. Jantunen, *Int. Mater. Rev.* 2008, **53**, 57.
5. I. M. Reaney & D. Iddles, *J. Am. Ceram. Soc.* 2006, **89**, 2063.
6. D. Zhou, D. Guo, W. B. Li, L. X. Pang, X. Yao, D. W. Wang, I. M. Reaney, *J. Mater. Chem. C.* 2016, **4**, 5357.
7. US 3938064 A, Devices using low loss dielectric material, Henry Miles O'Bryan, Jr., James Kevin Pluorde, John Thomson, Jr.
8. JR. H. M. O'Bryan, JR. J. Thomson, J. K. Plourde, *J. Am. Ceram. Soc.* 1974, **57**, 450.
9. S. Kawashima, M. Nishida, I. Ueda, H. Ouchi, *J. Am. Ceram. Soc.* 1983, **66**, 421.
10. D. J. Barber, K. M. Moulding, J. I. Zhou, *J. Mater. Sci.* 1997, **32**, 1531.
11. R. I. Scott, M. Thomas, C. Hampson, *J. Eur. Ceram. Soc.* 2003, **23**, 2467.
12. B. Jancar, D. Suvorov, M. Valant, G. Drazic, *J. Eur. Ceram. Soc.* 2003, **23**, 1391.
13. P. Sun, T. Nakamura, Y. J. Shan, Y. Inaguma, M. Itoh, T. Kitamura, *Jpn. J. Appl. Phys.* 1998, **37**, 5625.
14. S. Hirano, T. Hayashi, A. Hattori, *J. Am. Ceram. Soc.* 1991, **74**, 1320.
15. H. Ohsato, S. Nishigaki, T. Okuda, *Jpn. J. Appl. Phys.* 1992, **31**, 3136.
16. Murata, <http://www.murata.com/>
17. Kyocera, <http://global.kyocera.com/>
18. EPCOS, <https://en.tdk.eu/>
19. Trans-Tech, <https://www.transtech.com/>

20. R. D. Shannon, *J. Appl. Phys.* 1993, **73**, 348.
21. J. Y. Chen, W. H. Hsu, C. L. Huang, *J. Alloy Compd.* 2010, **504**, 284.
22. A. Templeton, X. Wang, S. J. Penn, S. J. Webb, L. F. Cohen, N. McN. Alford, J. *Am. Ceram. Soc.* 2000, **83**, 95.
23. D. Zhou, C. A. Randall, H. Wang, L. X. Pang, X. Yao, *J. Am. Ceram. Soc.* 2010, **93**, 1096.
24. D. K. Kwon, M. T. Lanagan, T. R. Shrout, *Mater. Lett.* 2007, **61**, 1827.
25. H. Ohsato, T. Tsunooka, Y. Ohishi, Y. Miyauchi, M. Ando, K. Kakimoto, *J. Korea Ceram. Soc.* 2003, **40**, 350.
26. M. T. Sebastian, *J. Eur. Ceram. Soc.* 2004, **24**, 2583.
27. M. A. Peña, J. L. G. Fierro, *Chem. Rev.* 2001, **101**, 1981.
28. B. Ullah, W. Lei, X. Q. Song, X. H. Wang, W. Z. Lu, *J. Eur. Ceram. Soc.* 2017, **37**, 3051.
29. M. H. Kim, J. B. Lim, S. Nahm, J. H. Paik, H. J. Lee, *J. Eur. Ceram. Soc.* 2007, **27**, 3033.
30. Ferro, <http://www.ferro.com/>.
31. Dupont, <http://www.dupont.com/>.
32. B. Muktha, M. H. Priya, G. Madras, T. N. Guru Row, *J. Phys. Chem. B* 2005, **109**, 11442.
33. P. V. Rysselberghe, *J. Phys. Chem.* 1932, **36**, 1152.
34. M. Tonouchi, *Nature Photon.* 2007, **1**, 97.
35. L. Duvillaret, F. Garet, J. L. Coutaz, *Appl. Opt.* 1999, **38**, 409.
36. S. Nashima, O. Morikawa, K. Takata, M. Hangyo, *J. Appl. Phys.* 2001, **90**, 837.
37. H. B. Hong, D. W. Kim, K. S. Hong, *Jpn. J. Appl. Phys.* 2003, **42**, 5172.
38. D. H. Kang, K. C. Nam, H. J. Cha, *J. Eur. Ceram. Soc.* 2006, **26**, 2117.

39. H. Kagata, T. Inoue, J. Kato, *Jpn. J. Appl. Phys.* 1992, **31**, 3152.
40. A. Borisevich, P. K. Davies, *J. Am. Ceram. Soc.* 2002, **85**, 2487.
41. B. Shen, X. Yao, L. Kang, D. Peng, *Ceram. Int.* 2004, **30**, 1203.
42. Q. Zeng, W. Li, J. L. Shi, J. K. Guo, H. Chen, M. L. Liu, *J. Eur. Ceram. Soc.* 2007, **27**, 261.
43. L. Li, X. M. Chen, *Mater. Lett.* 2009, **63**, 252.

Table 1. List of high k ($k > 60$) single phase LTCC materials with TCF $< \pm 40$ ppm/ $^{\circ}\text{C}$

Composition	Frequency (GHz)	S.T. ($^{\circ}\text{C}$)	ϵ_r	Qf (GHz)	TCF (ppm/ $^{\circ}\text{C}$)	Ref.
BaSm ₂ Ti ₄ O ₁₂ -16 mol.-%BaCu(B ₂ O ₅)	—	875	60	4,500	-30	29
Bi ₂ (Zn _{1/3} Ta _{2/3}) ₂ O ₇ -0.5 wt-%B ₂ O ₃	—	850	63.9	3,500	-14	37
Bi ₂ (Li _{0.5} Ta _{1.5})O ₇ -0.02Bi ₂ O ₃	4.3	920	64.1	11,200	-19	this work
LiNb _{0.6} Ti _{0.5} O ₃ -0.5 wt. % 0.17Li ₂ O-0.83V ₂ O ₅	5.92	850	64.7	5,900	+9.4	38
Li _{1-x-y} Nb _{1-x-y} Ti _{x-4y} O ₃ (x=0.1, y=0.1) -2 wt-%V ₂ O ₅	5.6	900	66	3,800	+11	39
Bi ₂ O ₃ -CaO-Nb ₂ O ₅ (52.5 :17.5 : 30)	3.6	925	66	330	+35	40
Bi ₂ (Zn _{1/3} Ta _{2/3}) ₂ O ₇	—	850	66.3	3,200	-8.8	41
LiNb _{0.6} Ti _{0.5} O ₃ -1 wt-%B ₂ O ₃	—	880	70	5,400	-6	42

Figure Captions:

Fig. 1 XRD patterns of the $\text{Bi}_2(\text{Li}_{0.5}\text{Ta}_{1.5})\text{O}_{7+x}\text{Bi}_2\text{O}_3$ ($x = 0, 0.01$ and 0.02) ceramics sintered at different temperatures and co-fired with $\text{Bi}_2(\text{Li}_{0.5}\text{Ta}_{1.5})\text{O}_{7+0.02}\text{Bi}_2\text{O}_3$ and 30 wt. % silver powders

Fig. 2 SEM images of the $\text{Bi}_2(\text{Li}_{0.5}\text{Ta}_{1.5})\text{O}_{7-x}\text{Bi}_2\text{O}_3$ for $x = 0$ sintered at $1025\text{ }^\circ\text{C}$ (a), $x = 0.01$ sintered at $1000\text{ }^\circ\text{C}$ (b), $x = 0.02$ sintered at $920\text{ }^\circ\text{C}$ (c), backscattered electron (BSE) image of co-fired ceramics with silver powders (d) and silver paste (e) sintered at $920\text{ }^\circ\text{C}$ and schematic of crystal structure (f)

Fig. 3 Microwave dielectric properties of the $\text{Bi}_2(\text{Li}_{0.5}\text{Ta}_{1.5})\text{O}_{7+x}\text{Bi}_2\text{O}_3$ ($x = 0, 0.01$ and 0.02) ceramics as a function of sintering temperature

Fig. 4 Real and imaginary parts of permittivity over a wide frequency range.

Fig. 5 Comparison of this work and commercial systems (a) for dielectric resonators and (b) high permittivity LTCC materials^{29,37-42}

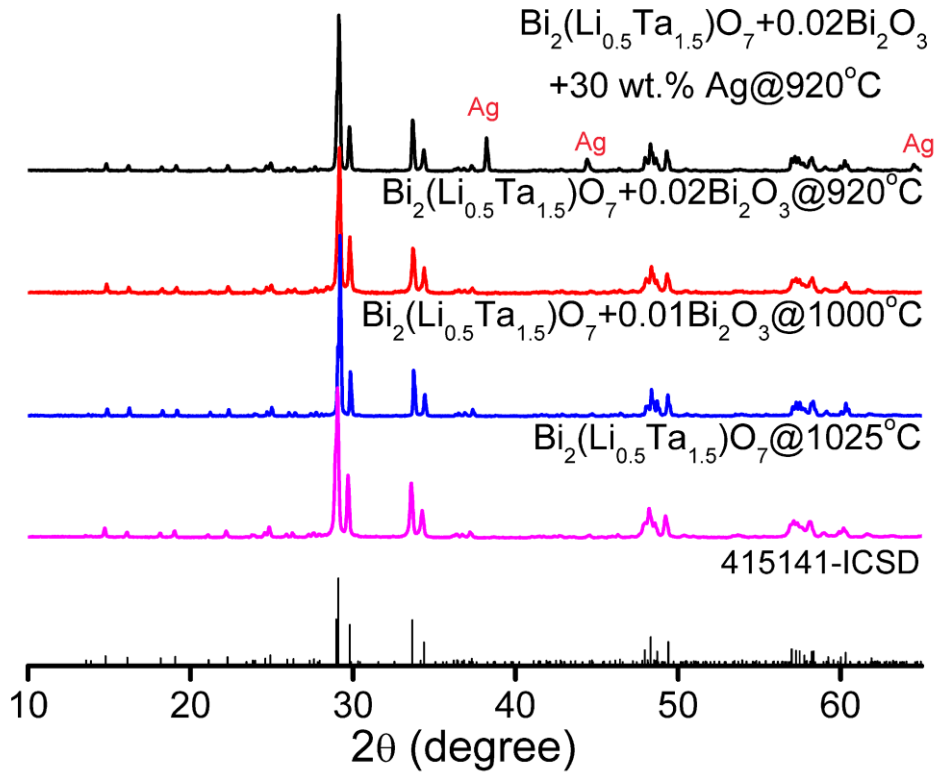


Fig. 1 XRD patterns of the $\text{Bi}_2(\text{Li}_{0.5}\text{Ta}_{1.5})\text{O}_{7+x}\text{Bi}_2\text{O}_3$ ($x = 0, 0.01$ and 0.02) ceramics sintered at different temperatures and co-fired with $\text{Bi}_2(\text{Li}_{0.5}\text{Ta}_{1.5})\text{O}_7 + 0.02\text{Bi}_2\text{O}_3$ and 30 wt. % silver powders

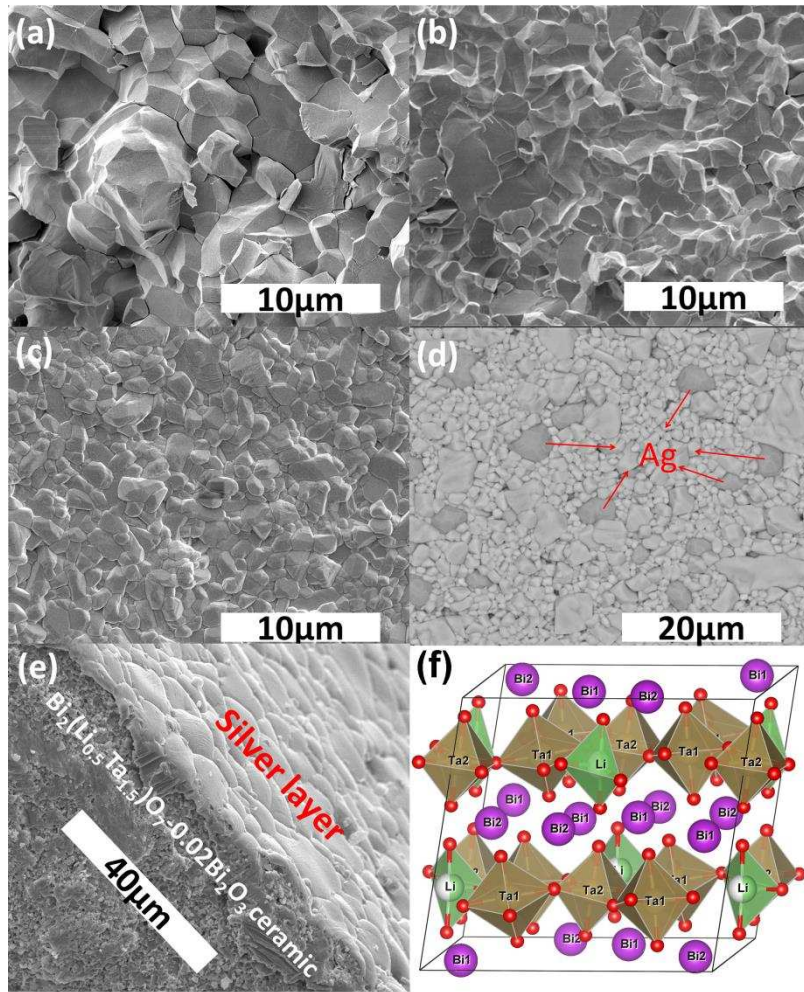


Fig. 2 SEM images of the $\text{Bi}_2(\text{Li}_{0.5}\text{Ta}_{1.5})\text{O}_{7-x}\text{Bi}_2\text{O}_3$ for $x = 0$ sintered at $1025\text{ }^\circ\text{C}$ (a), $x = 0.01$ sintered at $1000\text{ }^\circ\text{C}$ (b), $x = 0.02$ sintered at $920\text{ }^\circ\text{C}$ (c), backscattered electron (BSE) image of co-fired ceramics with silver powders (d) and silver paste (e) sintered at $920\text{ }^\circ\text{C}$ and schematic of crystal structure (f)

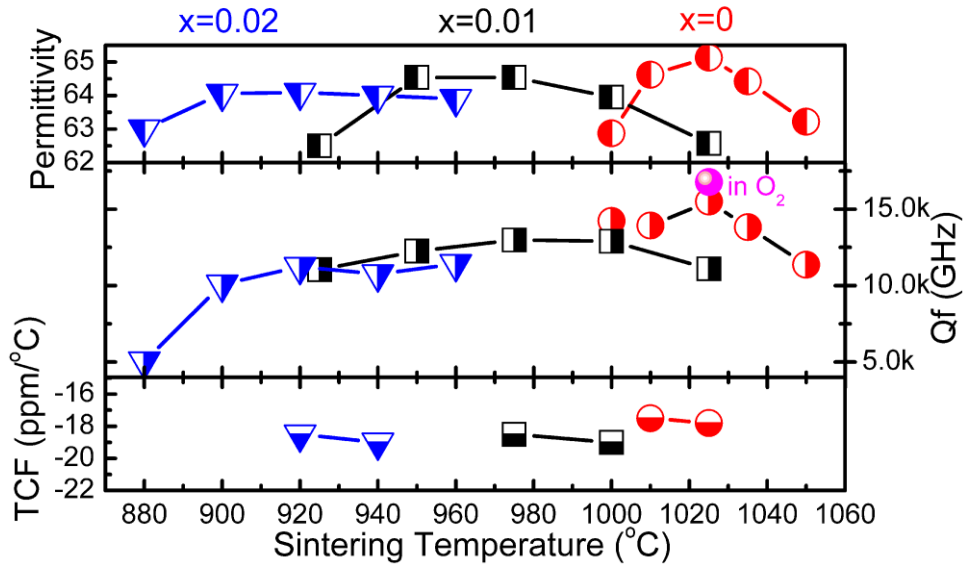


Fig. 3 Microwave dielectric properties of the $\text{Bi}_2(\text{Li}_{0.5}\text{Ta}_{1.5})\text{O}_{7+x}\text{Bi}_2\text{O}_3$ ($x = 0, 0.01$ and 0.02) ceramics as a function of sintering temperature

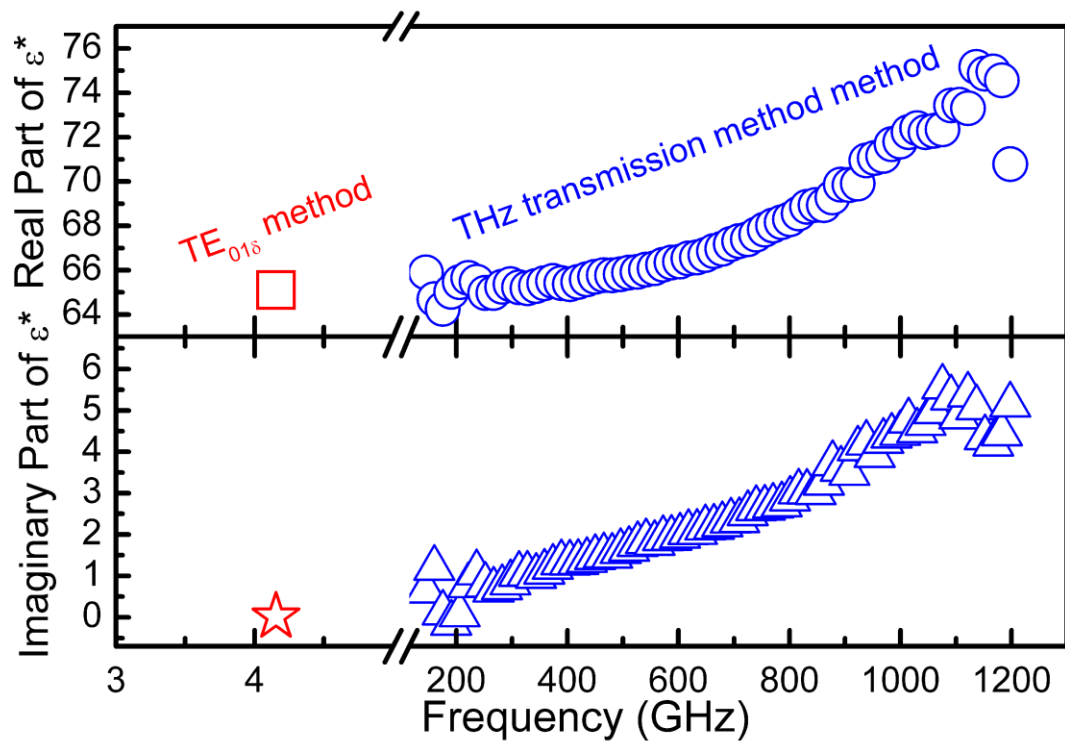


Fig. 4 Real and imaginary parts of permittivity over a wide frequency range.

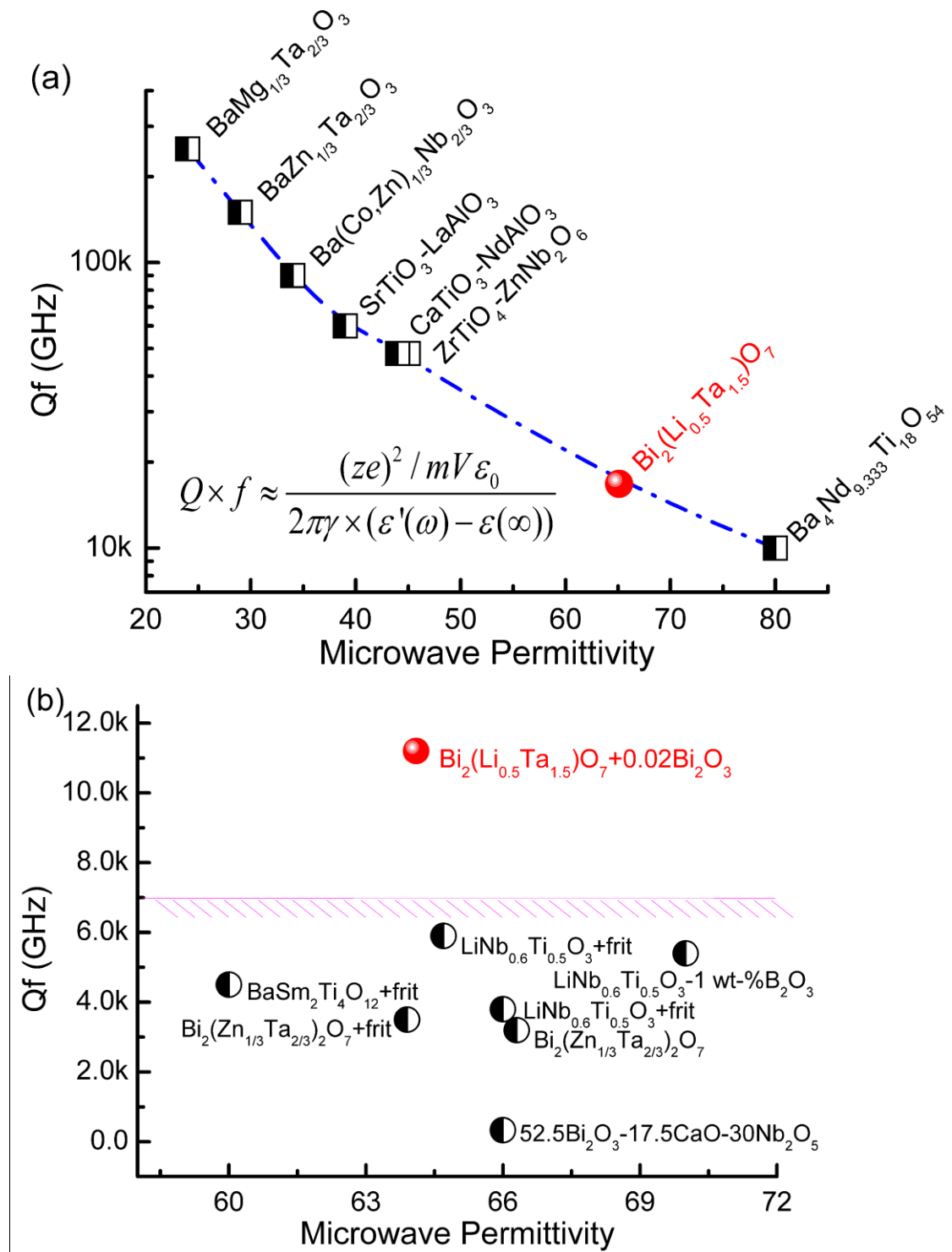


Fig. 5 Comparison of this work and commercial systems (a) for dielectric resonators and (b) high permittivity LTCC materials^{29,37-42}